Endothelial Shear Stress Enhancements: A Potential Solution for Critically Ill Covid-19 Patients

Sayed Nour (nourmd@mac.com)
https://orcid.org/0000-0002-3853-0942

Research Article

Keywords: Covid-19, Mechanical ventilation, Cardiopulmonary-circulatory assistance, Cardiac arrest, Endothelial function, Shear Stress

Posted Date: June 17th, 2020

DOI: https://doi.org/10.21203/rs.3.rs-35793/v1

Version of Record: A version of this preprint was published on December 3rd, 2020. See the published version at https://doi.org/10.1186/s12938-020-00835-7.

Endothelial Shear Stress Enhancements: A Potential Solution for Critically Ill Covid-19 Patients.

Sayed NOUR MD, PhD✉

Le LAB'O, Orleans Technopole, 1 avenue du Champs de Mars - 45074 Orleans France.

Short Title: Shear stress therapy in Covid-19.

✉ Corresponding author: Dr. Sayed Nour nourmd@mac.com

ID: https://orcid.org/0000-0002-3853-0942

Abstract

Rationale: Most critically ill Covid-19 patients succumb to multiple organ failure and / or cardiac arrest as a result of comorbid endothelial dysfunction disorders which had probably aggravated by conventional mechanical assist devices. Even worse, mechanical ventilators prevent the *respiratory pump* from performing its crucial function as a potential generator of endothelial shear stress (ESS) which controls microcirculation and hemodynamics since birth. The purpose of this work is to bring our experience with ESS enhancement and pulmonary vascular resistance (PVR) management as a potential therapeutic solution in acute respiratory distress syndrome (ARDS). We propose a noninvasive device composed of thoracic and infradiaphragmatic compartments that will be pulsated in an alternating frequency (20/40 bpm) with low-pressure pneumatic generator (0.1-0.5 bar). Oxygen supply, nasogastric ± endotracheal tubes are considered. **Proof-of-concept:** prototypes were tested in pediatric models of refractory cardiac arrest (≥20min), showed restoration of hemodynamics (BP≥100 mm Hg) and urine output, regardless of heartbeats, pharmacological supports and mechanical ventilation. **Conclusions** ESS enhancement represents a more effective treatment to increase tissue oxygenation and improve hemodynamic in ARDS. A cost-effective method which could be induced with a non-invasive pulsatile device adaptable to cardiopulmonary-circulatory biophysics to maintain a fully functional respiratory pump and avoid confrontation of the opposite hydraulic circuits.

Key Words: Covid-19 – Mechanical ventilation – Cardiopulmonary-circulatory assistance – Cardiac arrest – Endothelial function – Shear Stress.

Introduction

> "The great tragedy of Science is the slaying of a beautiful hypothesis by an ugly fact"
> **Thomas Huxley** [1].

Severe acute respiratory syndrome (SARS) has become a global healthcare issue over the last two decades [2].

Mechanical ventilation and pharmacological supports (e.g. vasopressors), are the conventional treatment for those who develop acute respiratory distress syndrome (ARDS).

Even though a number of devices and means adjunctive to conventional ARDS therapy, e.g. extracorporeal membrane oxygenation (ECMO), artificial kidney, … the survival rate still remains quite poor [3].

As yet, many predictions and controversies are still surrounding Covid-19 management, the disease still causes thousands of lives daily around the planet, regardless of healthcare progress.

Thus, fundamental and out-of-scope research is required in nearly all aspects of ARDS management.

Disadvantages of current ARDS management

As it is known, the human being is a multicellular organism in which cell biology plays a main role in terms of development, maintenance, proper functioning and also failure of vital organs. [4].

Maintaining good metabolic processes depend on organs' microcirculation which is controlled by plurality of endothelial mediators of vasodilators induced by shear stress of blood flow dynamics [5,6].

The therapeutic goal in a critically ill patient is to improve hemodynamics and tissue oxygenation in order to maintain healthy cellular metabolism to promote rapid recovery with restoring endothelial functions e.g., angiogenesis-apoptosis interdependency [7].

Meanwhile, once vital metabolic processes are threatened, regardless of the underlying pathology, it becomes a matter of resistance and fluid mechanics management.

Seemingly, relying on *systemic afterload* to improve hemodynamics, emerges a vicious cycle from endothelial dysfunction and momentum energy losses of opposing hydraulic circuits.

Taking the example of vasopressors that increase vascular resistance and myocardial oxygen consumption, most likely end in organ failure and mechanical assistance requirement. And this may explain that most of the deceased Covid-19 patients, had succumbed to comorbid endothelial dysfunction disorders, e.g., arterial hypertension, atherosclerosis (age), inflammatory response, immunosuppression, thromboembolic syndrome, … [8].

Based on our previous studies with endothelial shear stress [ESS] enhancement therapy, we have shown that *pulmonary afterload* controls *systemic afterload* and hemodynamics in pediatric models of cardiogenic shock [9].

Pressurized flow and shear rates are two constant endothelial stimulants that continue to regulate the closed hydraulic cardiovascular circuit since intrauterine life [10]

As shown in (Figure 1), the left ventricle (LV) and peristaltic arteries represent the main circulatory driving forces, at the left-heart side that contains less than 10% of blood volume [11], otherwise accessory forces are necessary to move up the massif volume (≥70%) of steady blood flow at the right-heart side such as the gravitational effect, the respiratory and muscle pumps [12], which become severely disturbed in bedridden ventilated patients.

The *respiratory pump* represents a low-pressure momentarily closed hydraulic circuit due to the epiglottis effect. It contains two types of fluids: Newtonian compressible (air) and non-Newtonian incompressible (blood) and is surrounded by two types of cells (endothelium and alveolar epithelium).

Physiologically, the *respiratory pump* squeezes the pulmonary parenchyma in an accordion-like manner, to release plenty of endothelial mediators to drop the pulmonary vascular resistances (PVR), to improve hemodynamics as well as tissue oxygenation with first breath after birth.

Functionally, the respiratory pump can redress hemodynamics and remedy the side effects of endothelial dysfunction caused by conventional CAD, which may explain long-term survival of continuous flow artificial-hearts transplants [13]. Also, an underdeveloped *respiratory pump* can explain failure of right heart bypass procedures in very young age [14].

Unfortunately, such an important role of the *respiratory pump* as a *master-key* circulatory driving force and a potential generator of ESS is still disregarded by therapists and seriously disturbed by ventilators. As ventilators with endotracheal intubation, neuromuscular blockade, transform the *respiratory pump* into a closed pressurized hydraulic circuit and promote serious complications, e.g., barotrauma, surinfection, … [15].

Apparently, ARDS patients exhibit shortness of breath despite mild hypoxia (PsaO2≤94%), which is normally uncompromising for life. On the other hand, patients with severe cyanosis, most often do not suffer from shortness of breath.

This undoubtedly means that ARDS patients are desperately in urgent need to increase the accordion-like maneuver of the *respiratory pump* and maintain the induction of pulmonary ESS to improve their hemodynamics and metabolic processes.
Alternatively, and as a potential solution, we propose endothelial shear stress (ESS) enhancement therapy for ARDS patients. Normally, ESS enhancement is the hallmark of physical exercise, which is induced physiologically to improve cardiac output (CO), organ performance, and general metabolic processes [16].

The proposed concept was presented at the American Thoracic Society conference in 2014 [17], and based on a *circulatory flow restoration* device, tested in pediatric models with sudden cardiac arrest [18].

Our main goal is to develop a low-pressure non-invasive cardiopulmonary-circulatory device capable of maintaining a full function of the *respiratory pump* to improve organs' perfusion-oxygenation and promote patients' recovery in better metabolic and hemodynamic conditions. This represents a cost-effective method and safer procedure compared to current therapies.

Materials and Methods

Principles of Endothelial Shear Stress (ESS) Therapy

The clinical applications of endothelial shear stress (ESS) with circulatory-assist devices (CAD) are controlled by several diversities between the cardiovascular system and lumped models [19]. While lumped models are constructed for driving a Newtonian compressible fluid inside

a closed pressurized hydraulic circuit, implementing rigid tubes with fixed diameter [20]. Meanwhile in practices a CAD is confronted with a non-Newtonian fluid (blood), running in flexible vessels with different geometries. This confrontation between two opposite pressurized hydraulic circuits creates a vicious circle of momentum energy losses manifested clinically by increased vascular resistances with endothelial dysfunction (e.g. hemorrhage, thromboembolism, inflammatory response, apoptosis, etc.), up till multiple organ failure.

Therefore, a CAD for ARDS management must adapt to pathophysiology and biophysics of the cardiopulmonary-circulatory system, maintain a fully functional *respiratory pump* and avoid opposite hydraulic circuits' confrontation.

Device

As represented in (Fig. 2), briefly, the device comprises one infradiaphragmatic pressure element (T1), one thoracic pressure element (T2), and pulsatile generator (G). In general, the chosen materials and design must allow attachment and/or wrapping of the device around the patient's body rapidly and tightly by therapists and adaptable to different body sizes (for further details please refer to patented description: US20140148739).

Once wrapped around the patient's body, an electro-mechanic pneumatic generator will induce the alternating pulsation between trunk and chest compartments (Fig. 3), in low-pressure (e.g., 0.1–0.5bars) and at fixed frequency of 40 bpm for the infradiaphragmatic element and 20 bpm for the thoracic vest.

The device could be synchronized and compatible with current mechanical ventilations security features. Selection of the best choice of oxygen supply will be determined by patient's conditions e.g., noninvasive ventilation (NIV) or endotracheal intubation in severe ARDS to allow bronchioalveolar lavage. In both conditions the device will not restrict the chest wall's mobility. A nasogastric tube must be considered. The automated device set function allows for handling additional medical instrumentations, as well as at-ease patients' inclination if requested.

Proof-of-concept

This study was approved by the Animal Research Facility at Sun Yat-Sen University and conformed to the Guide for the Care and Use of Laboratory Animals (NIH Publication No.85-23, Revised in 1996). A preliminary evaluating study was conducted at the Key Laboratory on Assisted Circulation, Ministry of Health of China, The First Affiliated Hospital of Sun Yat-sen University, Guangzhou, China. We followed the same anesthetic protocol, previously detailed in our various publications, cited in references.

As been previously described [18], prototypes (Fig. 4) were tested in pediatric animal models, (n° = 7 piglets and 4 puppies). Animals were premedicated with an anesthetic mixture composed of dihydroetorphine hydrochloride, dimethylaniline thiazole,

ethylenediaminetetraacetic acid, and haloperidol, (3 mL) and midazolam (0.5 mg/kg), given intramuscularly, then placed on a warmed operating table and surveyed with a rectal probe (38 ± 1 °C). Anesthesia was maintained by 3% sodium phenobarbital (1 mg/kg), divided into doses and mechanical ventilation. Through a median cervicotomy and tracheotomy, a 3.5–5 # tracheal tube was inserted, followed by mechanical ventilation (PA-500 PuLang Technologies Inc®) with 40% oxygen, 10–15 ml/kg min tidal volume and 15/min respiration frequency.

Hemodynamic monitoring, the right carotid artery was isolated, and a 6F catheter was introduced. Then a Millar probe (4F MIKRO-TIP catheter transducer; Millar Instruments) was introduced through the carotid line into the aorta for continuous systemic pressure (AP) monitoring (Biopac® physiology monitoring system). A 5F double-lumen central venous line (Hydrocath; BD Technologies), introduced through the right internal jugular vein for central venous pressure monitoring and IV fluids. Cerebral blood flow was measured with a Transonic transit-time flow meter ((Transonic Systems, Ithaca, NY, USA), positioned around the left carotid artery. Urine output was measured by urinary catheter in dogs and direct suprapubic catheter insertion in piglets. Peripheral cutaneous microcirculation was measured by a laser flowmeter (Perimed PeriScan PIM 3 System) positioned at the earlobe (piglet) or tongue (dog). All animals were mechanically ventilated through a tracheotomy tube.

*Procedures***,** animals were subjected to different methods of sudden cardiac arrest (SCA), e.g. potassium chloride (n°7), electric fibrillation (n°3), and asphyxia by clamping the tracheal tube (n°1). The cardiac arrest period was varied between 8 min (n°2), 20 min (n°3), and 30 min (n°4). Two animals (1 pig and 1 dog) were served as control survived standard CPR after 8 min of cardiac arrest (e.g., cardiac massage-DC shock-adrenaline). The pulsatile trousers prototype was pulsated at a low-pressure of 0.01 MPa and chest vest at 0.025 MPa and at the same frequency 40 bpm. The ventilation was switched off after cardiac arrest and restarted in the 2 controls after return of heartbeat. Ventilation remained switched off with the tracheal tube connected to oxygen bag in the entire treated group till the end of experiment.

TUNEL test: the myocardium of the treated asphyxiated dog was harvested and compared to a control dog, treated by conventional CPR after 8 min of cardiac arrest and kept alive for 6 h. The myocardial tissue was placed in 10% buffered formalin for 24 h, then mounted in paraffin and sectioned in 4 μm slices. The apoptotic cells were identified with a terminal deoxynucleotidyl transferase-mediated dUTP nick-end labeling (TUNEL) apoptosis detection kit according to the manufacturer's protocol (Boster Inc, China). Five photographs (magnification 20x) were taken of each tissue section. All TUNEL negative (blue) and TUNEL-positive (brown) nuclei were visualized under a light microscope; the total number of nuclei counted in 5 random high-power fields from each sample. The apoptotic index (AI) was calculated as 100% ∗ (TUNEL-positive nuclei / all nuclei).

Results

The spontaneous return of the heartbeat was almost instantaneous as soon as the device began operating in two piglets whose hearts stopped for 8 minutes.

In other animals with a longer cardiac arrest period (20-30 min), the device continued to operate for two hours without returning the heartbeat.

Nevertheless, there were significant improvement of hemodynamics data as depicted in (Fig. 5A–C): a nearly physiological aortic pressure curve with a systolic pressure greater than 100mm Hg and carotid echo Doppler greater than 300 m/s. There was restoration of renal function with massive urine output in all animals within 15 min of device pulsations and improvement of peripheral cutaneous microcirculation.

The TUNEL test showed inferior apoptotic cells in the treated dog as well as an obvious dilation of the intracardiac coronary vessels (Fig. 6A, B). There was global vasodilation, compensated by IV fluids (1–2 L).

Discussion

The outcomes of acute respiratory distress syndrome (ARDS) management remain insufficient with poor results, most probably due to patients' diversity and incompatibility of the applied methods with the pathophysiology and biophysics of the *respiratory pump*.

In contrast, the result of this study proved the feasibility and effectiveness of a circulatory flow restoration (CFR) device as a potential therapeutic method in ARDS. For the first time in the literature, we have shown that a low-pressure extracorporeal pulsatile device could induce a nearly physiological arterial pressure curve (Fig.5C) in cardiac arrest models, regardless of heartbeats. This means that the device's vest which is also served as a non-invasive mechanical ventilator, provided efficient cardiac compression and recoil of chest wall and promoted ESS of the respiratory pump. Similarly, the alternating pulsations delivered by the infradiaphragmatic element at the stagnant hepatic-splanchnic venous capacitance increased RV preload, during the vest inspiratory phase, and decreased pulmonary afterload. These were confirmed by significant improvements in hemodynamics data, the cutaneous microcirculation, myocardial apoptosis and urine output which required compensation with IV fluids, despite the state of cardiac arrest.

Endothelial Shear Stress Versus Conventional Therapy In ARDS

Most of ARDS patients present endothelial dysfunction comorbidities with increased pulmonary and systemic vascular resistances. A situation that most commonly worsen with conventional treatment such as vasopressors and steady-flow CADs like ECMO [21]. Yet, the immobilization of the *respiratory pump* and transformation of the respiratory tract into a closed pressurized hydraulic circuit by mechanical ventilators besides their interference with coronary perfusion flow are the principles causes of hemodynamic and metabolic deterioration in ARDS [21,22].

We have been previously reported the benefits of ESS applications in hemodynamic improvement with different pulsatile CAD tested in *acute cardiogenic shock* induced in *thirty-six* pediatric piglets divided equally (n=6) between groups, as follows (Table 1): Acute PAH, created with surgical aortopulmonary shunt [23]; Acute myocardial infarction (MI) [24], following permanent ligation of left anterior descending coronary artery (LAD) and Acute right ventricular failure (RVF) [25], following surgical disruption of pulmonary valve. As shown in (Table 2), there were significant improvement of hemodynamics and reduction of the pulmonary vascular resistances, within few minutes of device pulsations and without any pharmacological supports. In preclinical studies, low-pressure pulsatile devices, e.g. pulsatile trousers and mask prototypes, were tested on healthy volunteers, showed enhancement of the cutaneous microcirculation has also been observed, measured with a laser flowmeter (PeriFlux System 5000; Perimed) in an area remote from the pulsed zone (e.g. tip of the nose in mask trials, and fingertip with trousers) and increased cerebral blood flow (measured with carotid Doppler echo) after 20 min of un-synchronized pulsations (mask) [9,26].

Right-Heart Versus Left-Heart Endothelium

Contrary to historical consideration of endothelium as a homogenous cell layer, heterogeneity of the pulmonary endothelium is apparent and has been proven in literature from different disciplines [27]. In general, left heart side endothelial functions are most frequently explored and stimulated with devices, e.g., the intra-aortic balloon pump (IABP), etc. In the long-term, these left-heart side CAD usually show tolerant effects with further deterioration, rather than restoration, of endothelial function [28]. In contrast, our studies results proved the hypersensitivity of the pulmonary endothelium, which is a part of the right-heart, to shear stress stimuli. A few minutes of intrapulmonary catheter pulsations were more than enough to decrease a systolic PAP from ≥ 45 mmHg to approximately 9 mmHg within a few minutes (approximately 10) [23], which is contrary to IABP experience at the left heart side. Similar observations were obtained with the acute myocardial ischemia model [24]. However, in acute RV failure, an external pulsatile trouser, decreased RV pressure and PVR, albeit in a slightly longer time frame (approximately 20 min) [25].

Pulmonary Versus Systemic Vascular Resistance

Clinical applications of vasopressors to increase systemic vascular resistance for acute PAH management is currently recommended by intensivists [29]. A similar phenomenon is also observed with tetralogy of Fallot (TOF) cyanotic spells because the patient usually takes the advantage of the overriding aorta and assumes a squatting position to temporarily increase SVR in order to increase pulmonary flow dynamics of ESS to decrease PVR. However, hemodynamically that could be improved physiologically in a TOF patient, whose system may be deteriorated due to vasopressors (e.g., tachyarrhythmia, renal failure, multiple organ failure, etc.) [30].

In the previous studies, the effect of intrapulmonary shear stress enhancement was immediate on both SVR and PVR in the pulsatile group. Compared with vasopressors, there was evidence of increased renal flow without associated tachyarrhythmia, e.g., heart rate was 69 ± 19 bpm.

Endothelial Shear Stress-Microcirculation Interdependency

Endothelial shear stress (ESS)-microcirculation interdependency constitutes the cornerstone of the proposed concept.

While maintaining a full *respiratory pump* function, microcirculation behavior adapts to all circumstances of hematological disorders to ensure adequate tissue oxygenation by all means. For example, with a low or high hematocrit, the microcirculation exhibits a behavior that approximates that of Bernoulli's law, as interpreted by the Fahraeus-Lindqvist effect [31], in which plasma stuck at the inner vascular boundary layers while erythrocytes move faster at the center. This could explain the absence of cyanosis in anemic patients with low hematocrit, unlike those patients with high hematocrit, as erythrocytes aggregations at microcirculations induce cyanosis with clinical signs of finger clubbing (drumsticks fingers).

However, once the pulmonary production of ESS is compromised due to pathological conditions of the contractile structures of the respiratory pump, patients exhibit symptoms and signs such as tachycardia, tachyarrhythmia, orthopnea, ... which are pathophysiological accelerators of pulmonary ESS induction by the *respiratory pump* to improve microcirculation.

Endothelial Shear Stress Versus Conventional PAH Therapy

Current PAH management includes pharmacological supports such as: the nitrous oxide (NO)–cGMP pathway and the prostacyclin–cAMP and endothelin receptors antagonists [32]; inhalational NO (iNO) [33]; phosphodiesterase-5 (PDE5) inhibitors [34,35]. Nonpharmacological supports, along with the employment of mechanical-assist devices and/or surgical procedures, may be needed in critical hemodynamic cases [36].

Unfortunately, current PAH therapies remain insufficient linked with a dismal prognosis comparable with that of advanced cancer [37,38,39]. For example, iNO, which relaxes arterial smooth muscle in the absence of parenchymal lung disease, could increase endothelin-1 levels and decrease endogenous nitric oxide synthase (eNOS) activity [40]. Abrupt discontinuation of iNO can result in rebound PAH with further deterioration of hemodynamic [41, 42]. Similarly, inhaled iloprost, may cause acute bronchoconstriction [43,44]. These drawbacks of inhalational PAH therapies may be explained by the different behavior of the extra-alveolar and alveolar endothelial cells due to their different embryological origins [45].

The employment of CAD for PAH management is still linked with controversial results [46]. Unfortunately, CAD could aggravate hemodynamics, leading to multiple-organ failure due to factors linked to the devices themselves (e.g., momentum energy losses) or indirectly due to patient-related factors (e.g., age, sex, right or left heart failure, etc.). For example, devices that

unload and bypass the left ventricle are less successful when used at the RV, which is preload dependent.

In fact, PAH is an endothelial dysfunction disease, treated with pharmacological options which are functionally simulating what could be obtained naturally from the endothelium, but with side effects. Accordingly, we have induced ESS enhancement for PAH management with new generation of pulsatile circulatory assist devices (CAD) to reduce PVR and improve hemodynamics in a nearly physiological manner and without pharmacological supports.

Practically, a human body (Soma) can be divided into *three* imaginary hemorheological spheres [18]: **A**, **B**, and **C** (Somarheology theory), wherein A stands for the amount of fluids, that could be compressible Newtonian (e.g., air), or incompressible non-Newtonian (e.g., blood) fluids, surrounded by B, the barriers of cells (e.g., vascular endothelium, alveolar epithelium), overlapped by C, the covering tissues (e.g., vascular vessels, parenchyma, muscles, etc.). Therefore, reduction of pulmonary vascular resistances (PVR) could be induced with a pulsatile device *internally* through sphere (A) and/or *externally* e.g., through sphere (C) to create ESS at sphere (B), and in correspondence to the Dana Point (PAH) classification [47], as depicted in (Fig.7) [17].
For example, in group (C), e.g., Covid-19 patients with parenchymal congestion, delivery of ESS should be induced *externally* through sphere (C) with a pulsatile device adapted to patients' pathophysiological requirements.

As depicted in (Fig.3) the (CFR) device can induce ESS through several endothelial surrounding covering layers (C): parenchymal, mediastinal, thoracic cage muscles and the diaphragm.

As a result, the device stimulates the massive natural pulmonary and hepatic endothelial stocks, inducing plenty of mediators to restore hemodynamics and metabolic processes.

Contrarily to noninvasive ventilation (NIV), which is only considered in the early stages of SARS, the device can be used effectively in severe ARDS [48].

Unlike the iron lung [49], it is a low-pressure pulsatile device (0.1-0.5 bar), that can mobilize both supra and infradiaphragmatic structures of the respiratory pump that makes it suitable for all ages and genders without side effects, e.g., rib fractures, mammary glands hematoma,

The device is an automated assembly that could be easily tilted at the request of clinicians, e.g., physiotherapists. Therefore, it could be an exclusive therapeutic tool for ARDS and achievement of current concept-based trials that showed some hope, but still remain without major impacts, e.g., prone position, low-dose neuromuscular blockades, thrombolytics therapies… [50].

Study limits

We have been confronted with some technical difficulties that include the use of two separate mal-synchronized pneumatic generators. A tissue prototype, which is less rigid at its outer part that makes the body compression less efficient particularly, with the morphological difference between the dog and the pig that required specific prototypes for each model.

Perspectives

We have planned to continue the development pathway of the CFR, as has been figured recently from the United States Food and Drug Administration [51], with preclinical studies for out of hospital cardiac arrest management. We have planned a PAH study in hypoxic piglets' model. Both programs are in standby for logistic, unscientific reasons.

Nevertheless, given the current pandemic with the shortage and/or controversial results of ventilators worldwide, in review with the FINER criteria for a good research question and the phases of evaluation of new therapies [52,53], we consider a low-pressure noninvasive device is ease of manufacture, safe for use to promotes endothelial shear stress to improve hemodynamic, tissues oxygenation and metabolic processes, which significantly will improve the outcomes of critically ill Covid-19 patients.

Conclusion: Compared with traditional therapies, ESS enhancement represents a more effective treatment to decrease PVR and improve hemodynamic in ARDS. This method could be induced properly with pulsatile CAD adaptable for pathophysiology and biophysics of *three* hemorheological spheres (ABC) that may assemble the several forms of the disease.

Acknowledgments: We express our gratitude to our Former Teachers, Dear Colleagues and Friends from: HEGP, and Marie-Lannelongue Hospitals, Paris, France; and the University of Sun Yat Sen, GZ; China. We acknowledge the precious support of Bpifrance, Conseil Regional and Technopole, Central Region, France.

Conflict of Interest: None declared.

References:

1. Huxley TH. Biogenesis and abiogenesis. *NATURE*; 1870 **2**: 400-407.
2. LeDuc JW, Barry MA. SARS, the first pandemic of the 21st Century. *Emerg Infect Dis*; 2004 **10**: 26.
3. Combes A, Hajage D, Capellier G, et al. Extracorporeal membrane oxygenation for severe acute respiratory distress syndrome. *N Engl J Med;* 2018 **378**:1965-75.
4. Samet I, Lelkes PI. Mechanical forces and endothelium. 2-11 (Harwood academic publishers, The Netherlands, 1999).
5. Neri Serneri GG. Pathophysiological aspects of platelet aggregation in relation to blood flow rheology in microcirculation. *Ric Clin Lab;* 1981 **11**: 39–46.
6. Koller A, Kaley G. Endothelium regulates skeletal muscle microcirculation by a blood flow velocity-sensing mechanism. *Am J Physiol;* 1990 **258**: 916-20.
7. Koh TJ, DiPietro LA. Inflammation and wound healing: the role of the macrophage. *Expert Rev Mol Med*; 2011 **13**: e23.
8. Behnood B. et al. COVID-19 and Thrombotic or thromboembolic disease: Implications for prevention, antithrombotic therapy, and follow-up. *J Am Coll Cardiol*; 2020 doi: 10.1016/j.jacc.2020.04.031.
9. Nour S. New hemodynamic theory "Flow and Rate": Concept and clinical applications using new pulsatile circulatory assist devices. PhD Thesis; Therapeutic Innovations, University Paris Sud - Paris XI, 2012. Français. ⟨NNT :2012PA114862).
10. Li Y, Zheng J, Bird IM, Magness RR. Effects of pulsatile shear stress on signaling mechanisms controlling nitric oxide production, endothelial nitric oxide synthase phosphorylation, and expression in ovine fetoplacental artery endothelial cells. *Endothelium*; 2005 **12**: 21–39.
11. Nour S, Liu J, Dai G, et al. Shear stress, energy losses and costs: a resolved dilemma of pulsatile cardiac assist devices. *Biomed Res Int*; 2014 **2014**: 651769-12.
12. Nour S, Wu G, Zhensheng Zh, et al. The forgotten driving forces in right heart failure: concept and device. Asian *Cardiovasc Thorac Ann*; 2009 **17**: 525-30.
13. Slaughter MS. Long-term continuous flow left ventricular assist device support and end-organ function: prospects for destination therapy. *J Card Surg*; 2010 **25**: 490-4.
14. Giglia TM, Humpl T. Preoperative pulmonary hemodynamics and assessment of operability: is there a pulmonary vascular resistance that precludes cardiac operation? *Pediatr Crit Care Med*; 2010 **2**: 57-69.
15. Ioannidis G, Lazaridis G, Baka S, et al. Barotrauma and pneumothorax. *J Thorac Dis*; 2015 **7**: 38-43.
16. Aaron CP, Tandri H, Barr RG, et al. Physical activity and right ventricular structure and function. The MESA Right Ventricle Study. *Am J Respir Crit Care Med*; 2011 **183**: 396–404.
17. Nour S. Fiction mirrors truth! The ABC target-board for pulmonary arterial hypertension. C53. Clinical evaluation and biomarkers of pulmonary hypertension II. *ATS* A4780-A4780 (2014).

18. Nour S, Carbognani D, Chachques JC. Circulatory flow restoration versus cardiopulmonary resuscitation: new therapeutic approach in sudden cardiac arrest. *Artif Organs*; 2017 **41**: 356-366.
19. Olufsen MS, Nadim A. On deriving lumped models for blood flow and pressure in the systemic arteries. *Math Biosci Eng*; 2004 **1**: 61–80.
20. Roselli RJ, Brophy SP. Redesigning a biomechanics course using challenge-based instruction. *IEEE Eng Med Biol Mag*; 2003 **22**: 66–70.
21. SOS-KANTO study group. Comparison of arterial blood gases of laryngeal mask airway and bag-valve-mask ventilation in out-of-hospital cardiac arrests. *Circ J*; 2009 **73**: 490–6.
22. Cooper JA, Cooper JD, Cooper JM. Cardiopulmonary resuscitation: history, current practice, and future direction. *Circulation*; 2006 **114**: 2839–49.
23. Nour S, Dai G, Carbognani D, et al. Intrapulmonary shear stress enhancement: A new therapeutic approach in pulmonary arterial hypertension. *Pediat Cardiol*;2012 **33**: 1332-42.
24. Nour S, Yang D, Dai G, et al. Intrapulmonary shear stress enhancement: A new therapeutic approach in acute myocardial ischemia. *Int J Cardiol*; 2013 **168**: 4199-208.
25. Nour S, Dai G, Wang Q, et al. Forgotten driving forces in right heart failure (Part II): Experimental study. *Asian Cardiovasc Thorac Ann*; 2012 **20**: 646-657.
26. Nour S. Flow and rate: concept and clinical applications of a new hemodynamic theory. Ch.17–76 (Misra ed., A.N. Biophysics. Intech, Rijeka 2012).
27. Ochoa CD, Wu S, Stevens T. New developments in lung endothelial heterogeneity: Von Willebrand factor, P-selectin, and the Weibel-Palade body. *Semin Thromb Hemost*; 2010 **36**: 301–308.
28. Scholz KH. Reperfusion therapy and mechanical circulatory support in patients in cardiogenic shock. *Herz*; 1999 **24**: 448–464.
29. Thomas M. Management of pulmonary hypertension in the intensive care unit. *Crit Care Med*; 2008 **36**: 651–652.
30. Zamanian RT, Haddad F, Doyle RL. & Weinacker, A.B. Management strategies for patients with pulmonary hypertension in the intensive care unit. *Crit Care Med*; 2007 **35**: 2037–2050.
31. Fahraeus R, Lindquist T. The Viscosity of the blood in narrow capillary tubes. *Am J Physiol, Vol*;1931 **96**: 562-568.
32. Boutet K, Montani D, Jaïs X. Review: therapeutic advances in pulmonary arterial hypertension. *Ther Adv Respir Dis*; 2008 **2**: 249–265.
33. Checchia PA, Bronicki RA, Goldstein B. Review of inhaled nitric oxide in the pediatric cardiac surgery setting. *Pediatr Card*; 2012 **33**: 493-505.
34. Tessler RB, Zadinello M, Fiori H, et al. Tadalafil improves oxygenation in a model of newborn pulmonary hypertension. *Pediatr Crit Care Med*; 2008 **9**: 330–332.
35. Nemoto S, Sasaki T, Ozawa H, et al. Oral sildenafil for persistent pulmonary hypertension early after congenital cardiac surgery in children. *Eur J Cardiothorac Surg*; 2010 **38**: 71–77.
36. McLaughlin VV, Benza RL, Rubin LJ, et al. Addition of inhaled treprostinil to oral therapy for pulmonary arterial hypertension: a randomized controlled clinical trial. *J Am Coll Cardiol*; 2010 **55**: 1915–1922.

37. Humbert M, Morrell NW, Archer SL. Cellular and molecular pathobiology of pulmonary arterial hypertension. *J AmColl Cardiol*; 2004 **43**: 13–24.
38. Felker GM, Thompson RE, Hare JM, et al. Underlying causes and long-term survival in patients with initially unexplained cardiomyopathy. *N Engl J Med*; 2000 **342**: 1077–1084.
39. Nef HM, Möllmann H, Hamm C. Pulmonary hypertension: updated classification and management of pulmonary hypertension. *Heart*; 2010 **96**: 552–559.
40. Macchia A, Marchioli R, Marfisi R. A meta-analysis of trials of pulmonary hypertension: a clinical condition looking for drugs and research methodology. *Am Heart J*; 2007 **153**: 1037–1047.
41. Bush A. Pulmonary and critical care updates (update in pediatrics 2005). *Am J Respir Crit Care Med*; 2006 **173**: 585–592.
42. Oishi P, Grobe A, Benavidez E. Inhaled nitric oxide induced NOS inhibition and rebound pulmonary hypertension: a role for superoxide and peroxynitrite in the intact lamb. *Am J Physiol Lung Cell Mol Physiol*; 2006 **290**: 359–366.
43. Miller OI, Tang SF, Keech A, et al. Rebound pulmonary hypertension on withdrawal from inhaled nitric oxide [letter]. *Lancet*; 1995 **346**: 51–52.
44. Segal ES, Valette C, Oster L. Risk management strategies in the postmarketing period: safety experience with the US and European Bosentan Surveillance Programmes. *Drug Saf*; 2005 **28**: 971–980.
45. Stevens T. Lung vascular cell heterogeneity: endothelium, smooth muscle, and fibroblasts. *Proc Am Thorac Soc*; 2008 **5**: 783–791.
46. Martin J, Siegenthaler MP, Friesewinkel O. Implantable left ventricular assist device for treatment of pulmonary hypertension in candidates for orthotopic heart transplantation—a preliminary study. *Eur J Cardiothorac Surg*; 2004 **25**: 971–977.
47. Simonneau G, Robbins IM, Beghetti M, et al. Updated clinical classification of pulmonary hypertension. *JACC*; 2009 **54**: 43-54.
48. Lau AC, Yam LY, So LK. Management of critically ill patients with severe acute respiratory syndrome (SARS). *Int J Med Sci*; 2004 **1**: 1-10.
49. Goti P, Duranti R, Spinelli A, et al. Effects of the iron lung on respiratory function in chronic hypercapnic COPD patients. *Arch Chest Dis*; 1995 **50**: 427-32.
50. Scholten EL, Beitler JR, Prisk GK, et al. treatment of ARDS with prone positioning. *Chest*; 2017 **151**: 215-224.
51. Guan A, Hamilton P, Wang Y, et al. Medical devices on chips. *Nat Biomed Eng*; 2017 **1**: 45–10.
52. Hulley SB, Cummings SR, Browner WS, et al. Designing clinical research. (4th ed. Philadelphia: Lippincott Williams & Wilkins; 2013).
53. Pocock S J, Clayton TC, Stone DW. Challenging issues in clinical trial design Part 4 of a 4-part series on statistics for clinical trials. *Jam Coll Cardiol*; 2015 **66**: 2886-2898.

Figure legends

Figure 1: Biophysics of cardiopulmonary circulatory driving forces. I: Right heart circuit main remodeling zones: Z1, systemic veins; Z2, right ventricle; Z3, septum; Z4, infundibulum; Z5, pulmonary artery [ref.]. II: Respiratory pump; a semiclosed pressurized circuit that compresses two types of fluids: Newtonian (air) and non-Newtonian (blood), in an accordion-like manner, creating ESS. III: Left heart circuit main remodeling zones: Z1, left ventricle; Z2, Aorta & Valsalva. IV: Mechanical ventilator: creates a nonphysiological immobilized closed pressurized respiratory circuit with suppression of ESS. V: CFR device that could restore circulatory flow dynamics and maintain respiratory pump function. [Artif Organs, Vol. 41, No. 2, 2017].

Figure 2: Shows the Circulatory flow restoration (CFR) device in a suitcase (middle panel) that contains (right panel): Vest (T2), abdominal corset (T1) and Console of commands (G). Left panel: a wrapped device around a patient on a deployed medical stretcher suitcase.

Figure 3: A schema representing the mechanism of the alternating compression/decompression the thoracic (T2) and abdominal (T1) compartments of the CFR device. The upper panel shows the CFR in an inspiration phase. The Lower panel shows the CFR in an expiration phase. C= covering endothelial layer shearing zone; C-1= thoracic cage; C-2= mediastinal shearing mass; C-3= pulmonary parenchyma, C-4= diaphragmatic pump; C-5 = hepatosplanchnic shearing mass.

Figure 4: Thoracic vest and trousers prototype wrapped around piglet body and connected to pneumatic generator [Artif Organs, Vol. 41, No. 2, 2017].

Figure 5A: Hemodynamic data obtained in a pediatric cardiac arrest model at baseline, showing ECG readings (upper line), aortic pressure line (middle curve) and carotid flow
Figure 5B: Post cardiac arrest hemostatic data.
Figure 5C: Restoration of hemodynamics with CFR device in a pediatric model after 30 min of cardiac arrest by asphyxia [Artif Organs, Vol. 41, No. 2, 2017].

Figure 6A: TUNEL test showing manifestation of myocardial apoptotic cells (blue color) in control.
Figure 6B: TUNEL test showing few manifestations of myocardial apoptotic cells (blue color) with vasodilation of intramyocardial vessels in tested in puppy (asphyxia model) after 2 h of device pulsations [Artif Organs, Vol. 41, No. 2, 2017].

Figure 7: Dana Point vs. ABC Target-Board Pulmonary Hypertension Management [17].
Right panel: Schematic imaginary division of the human body into three rheological spheres (A, B and C): A = amount of fluid; B = barriers of cells; C = covering tissues; "Somarheology theory" [18]. Middle panel Dana Point PAH classification [47]. Left panel: mismatching the Dana Point groups of PAH & ABC spheres. Endothelial shear stress could be triggered at **B**, through **A** and/or **C**.

Tables

Table 1: Endothelial shear stress therapy versus conventional in cardiogenic shock models [23-25].

Model	Surgical Procedure	Pulsatile CAD	Control
Acute MI	Permanent LAD ligation	Intrapulmonary catheter	Nitrates
Acute PAH	Ao-pulm shunt	Intrapulmonary catheter	Tadalafil
Acute RVF	Pulm valve avulsion	Pulsatile trousers	Adrenaline, IV fluid, Tadalafil

MI: myocardial ischemia; PAH: pulmonary arterial hypertension; RVF: right ventricular failure; Ao-pulm: aortico- pulmonary artery shunt, LAD: left anterior descending coronary artery, Pulm: pulmonary.

Table 2: Results of hemodynamic data of both groups: pulsatile and control (n=36)*.

	Pulsatile		Control	
Models	**PVRI**	**CO**	**PVRI**	**CO**
Acute MI	119±13	0.92±0.15	400±42	0.52±0.08
Acute PAH	85.8±42.12	0.56 ±0.26	478.6±192.91	0.54 ±0.11
Acute RVF	174±60	1±0.2	352±118	0.7±0.2

Groups: pulsatile (n=18) and control (n=18); MI: myocardial ischemia; PAH: pulmonary arterial hypertension; RVF: right ventricular failure; PVRI: pulmonary vascular resistances index (dyne.sec/cm^{-5}.kg^{-1}); CO: cardiac output (L/min); $p<0.05$ (2 ways-ANOVA)*.

Figure 1:

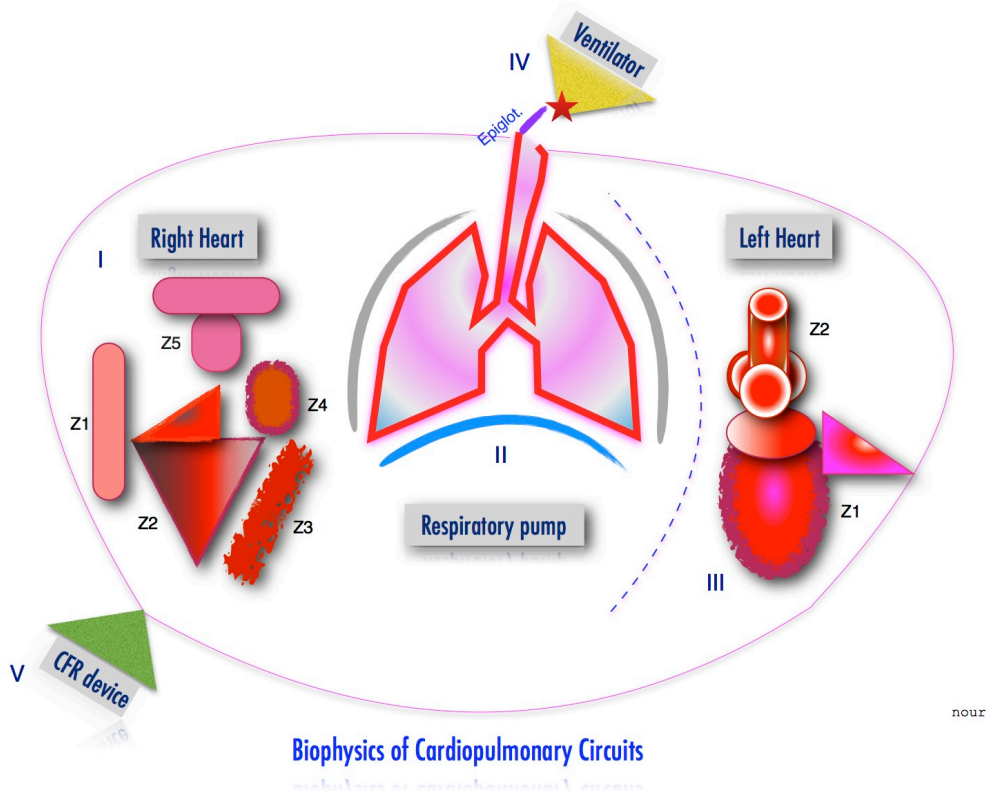
IV
Ventilator
Epiglot.
I
Right Heart
Z5
Z1
Z4
Z2
Z3
II
Respiratory pump
Left Heart
Z2
Z1
III
V
CFR device
nour
Biophysics of Cardiopulmonary Circuits

Figure 2:

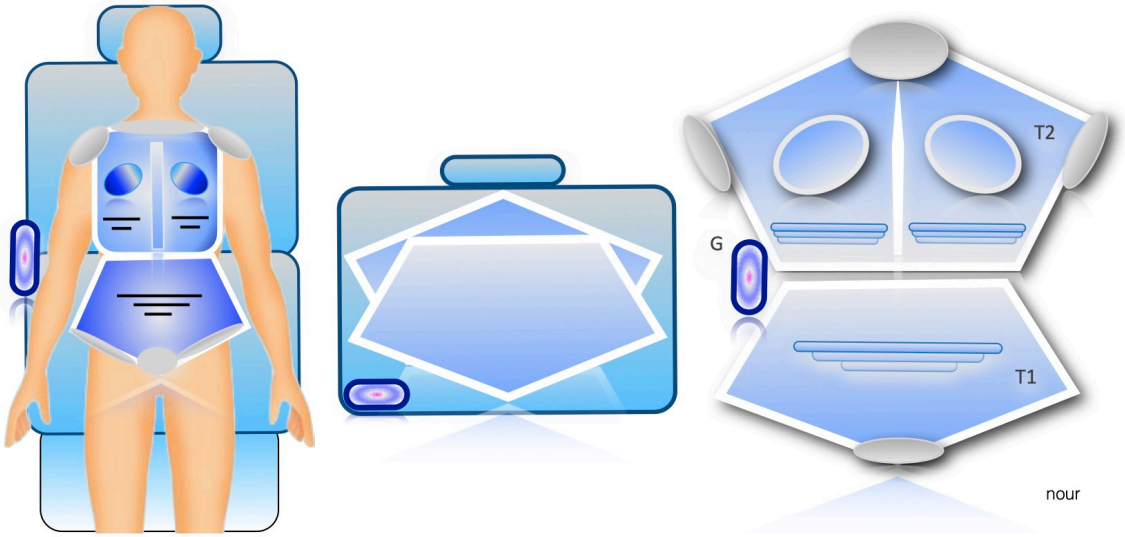

Figure 3:

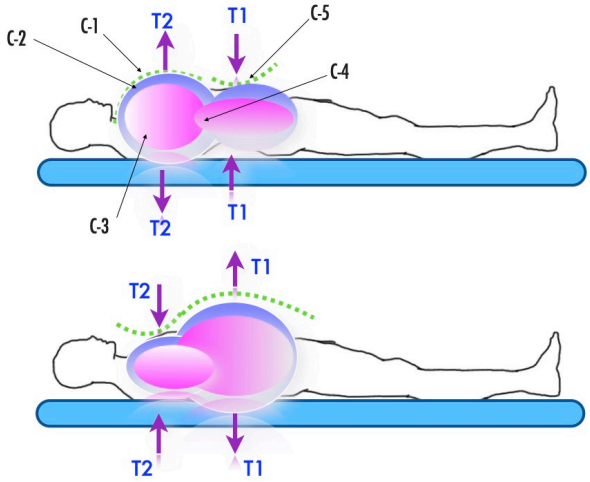

nour

Figure 4:

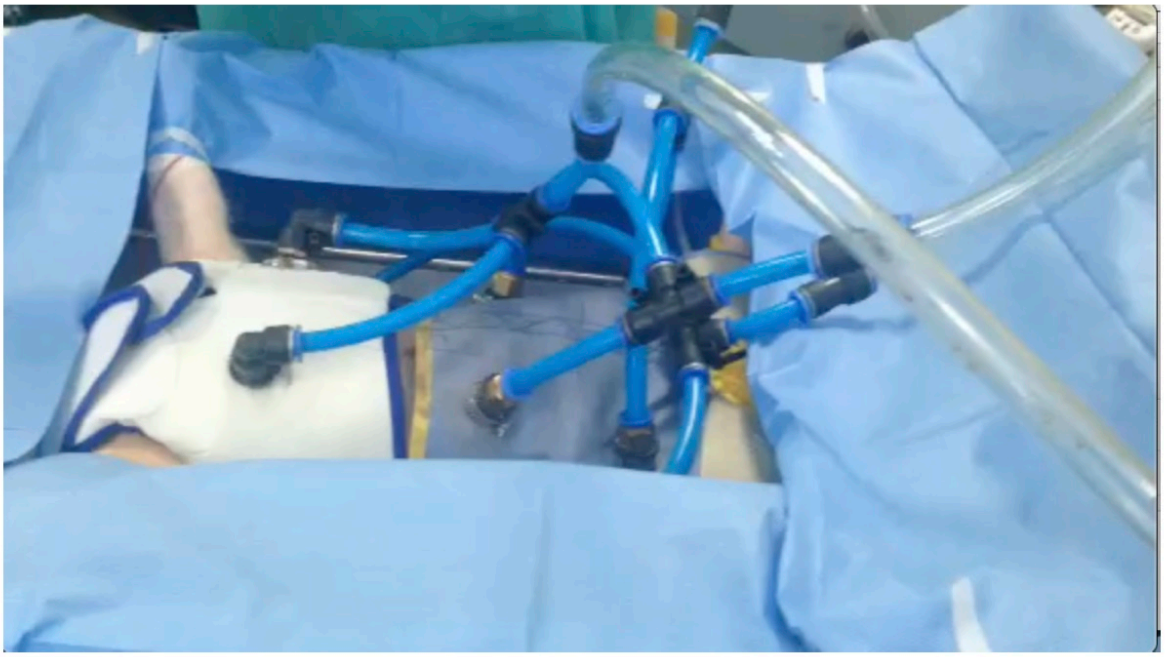

Figure 5A:

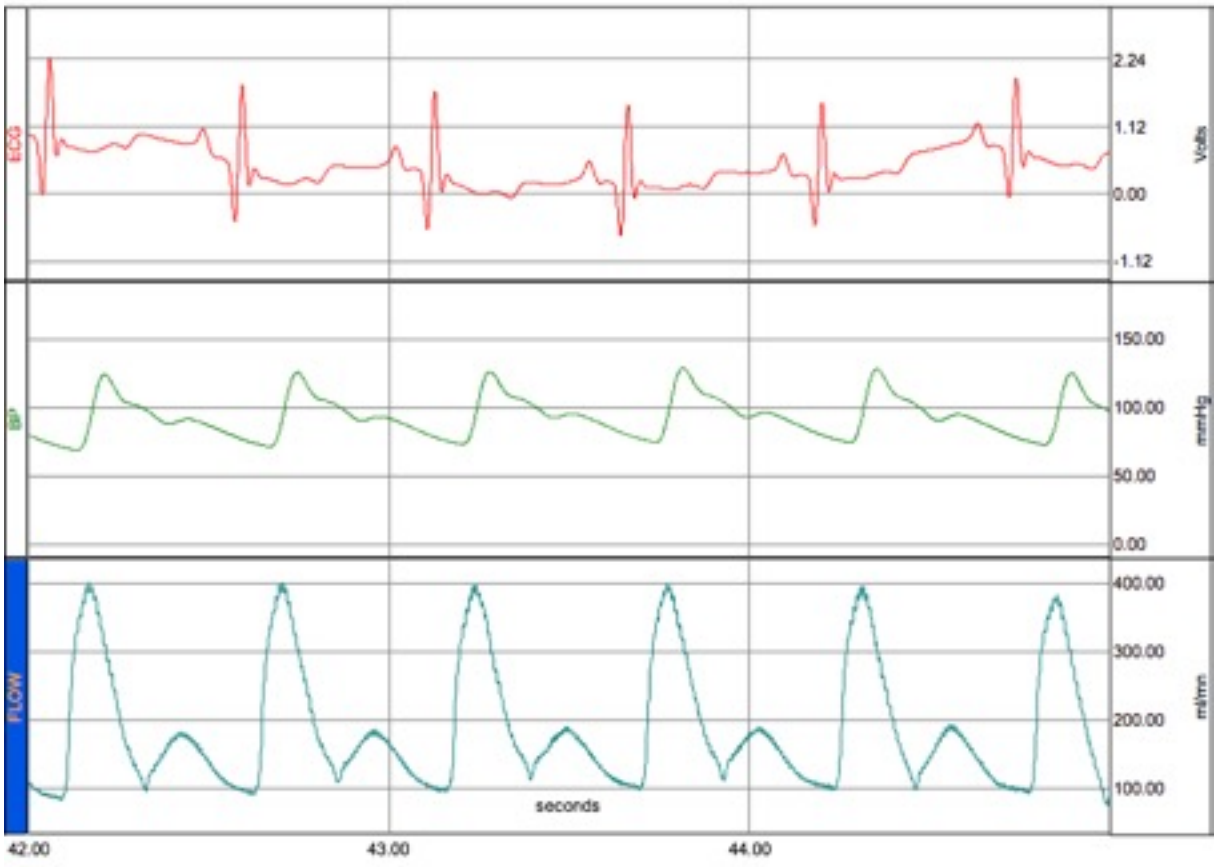
ECG
2.24
1.12
0.00
-1.12
Volts
BP
150.00
100.00
50.00
0.00
mmHg
FLOW
400.00
300.00
200.00
100.00
ml/m
seconds
42.00
43.00
44.00

Figure 5B:

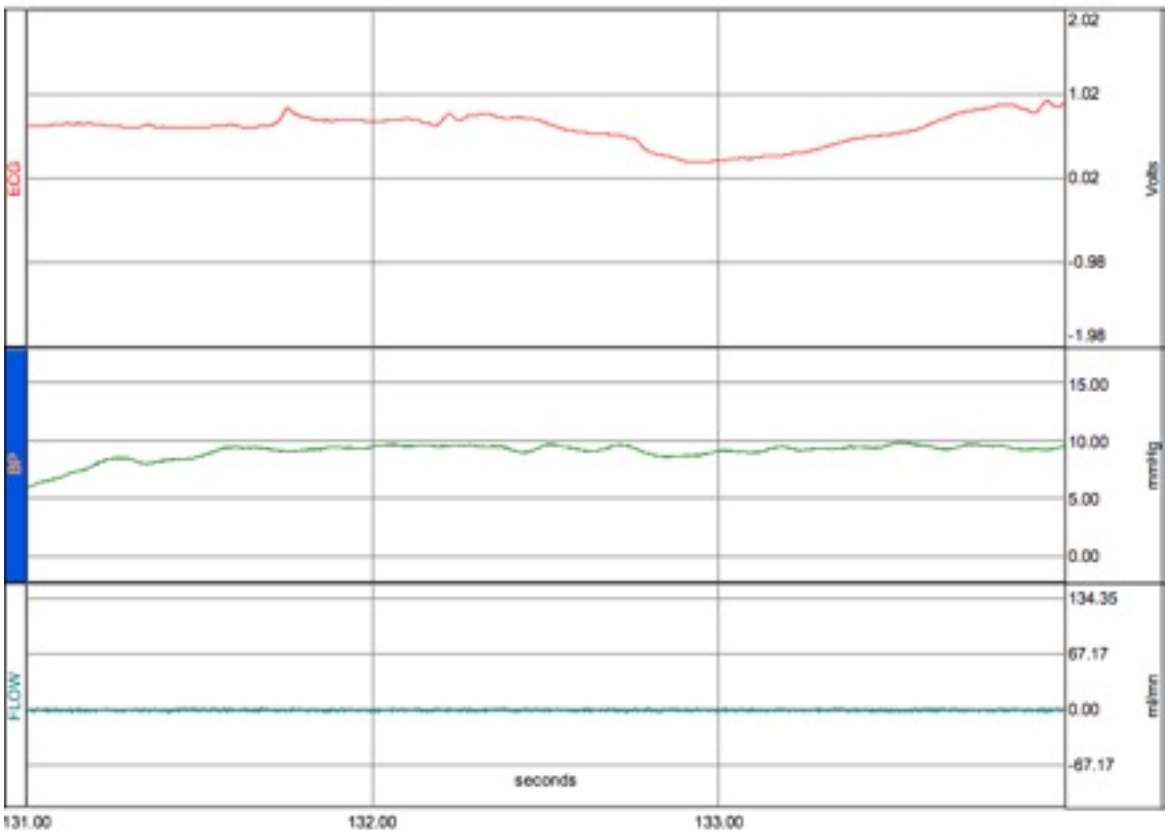
ECG
2.02
1.02
0.02
-0.98
-1.98
Volts
BP
15.00
10.00
5.00
0.00
mmHg
FLOW
134.35
67.17
0.00
-67.17
ml/mn
seconds
131.00
132.00
133.00

Figure 5C:

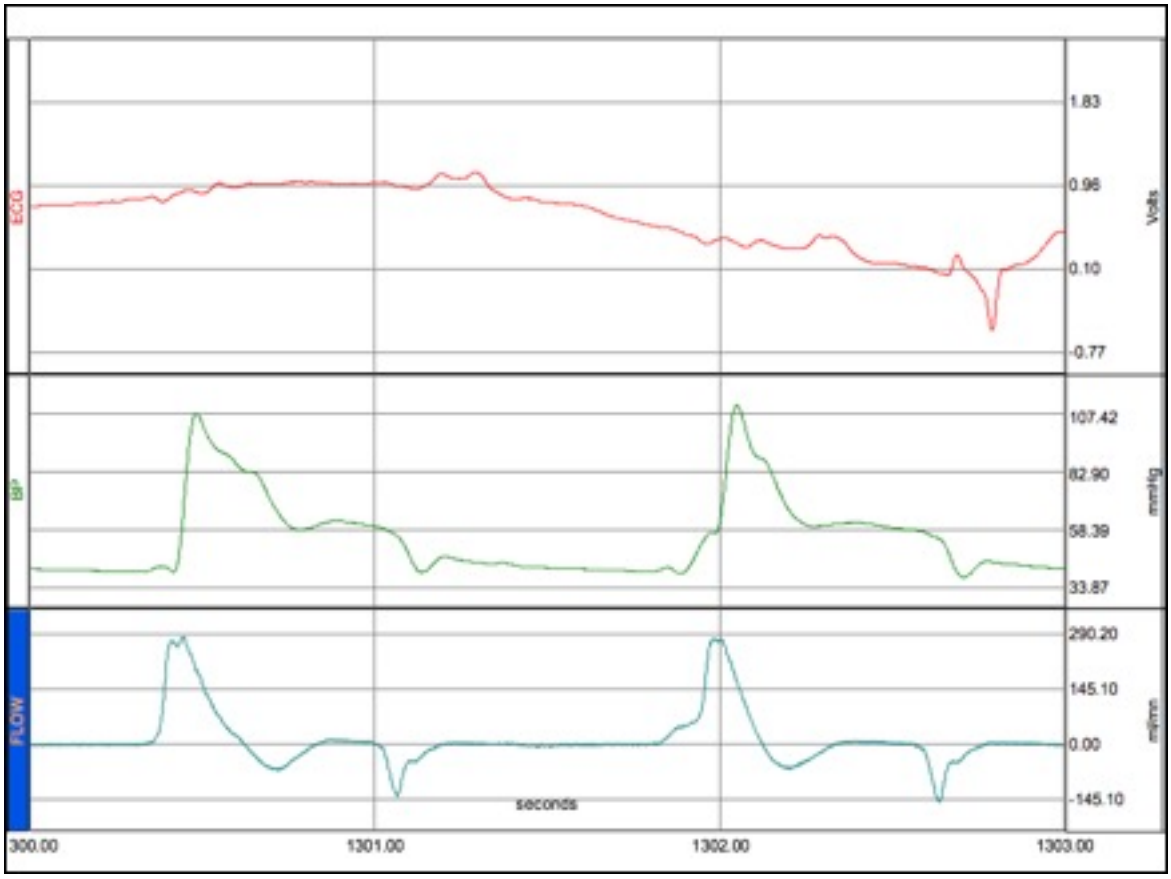
ECG
1.83
0.96
0.10
-0.77
Volts
BP
107.42
82.90
58.39
33.87
mmHg
FLOW
290.20
145.10
0.00
-145.10
l/min
seconds
300.00
1301.00
1302.00
1303.00

Figure 6A:

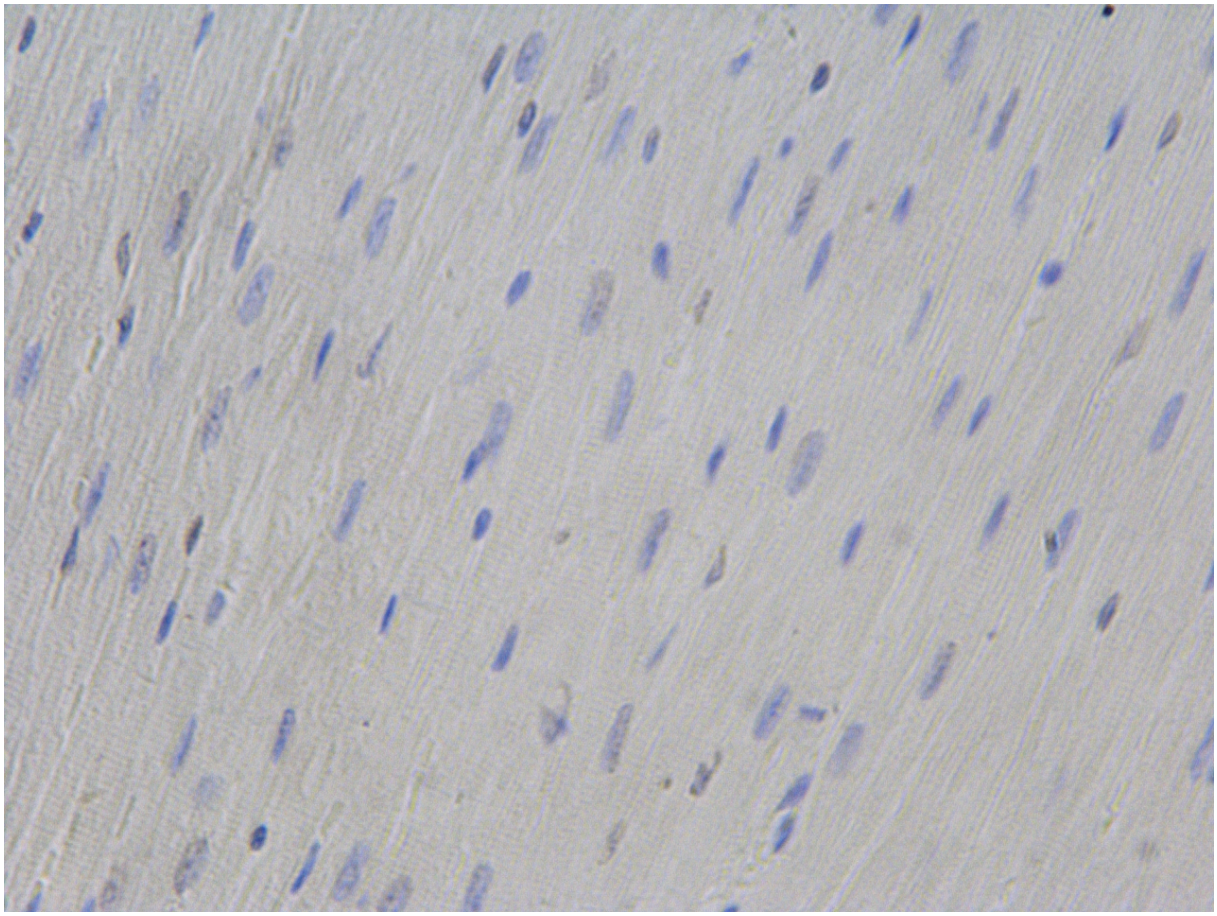

Figure 6B:

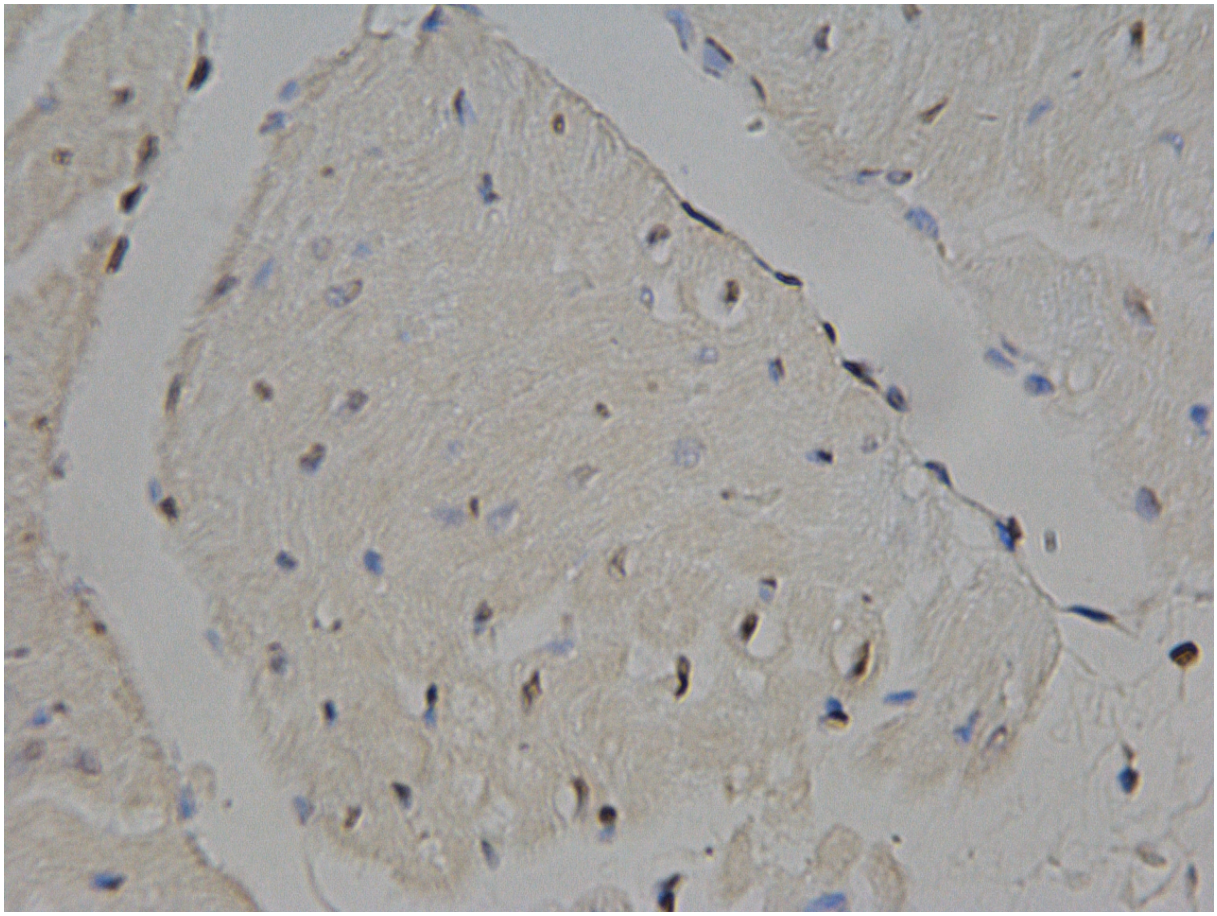

Figure 7:

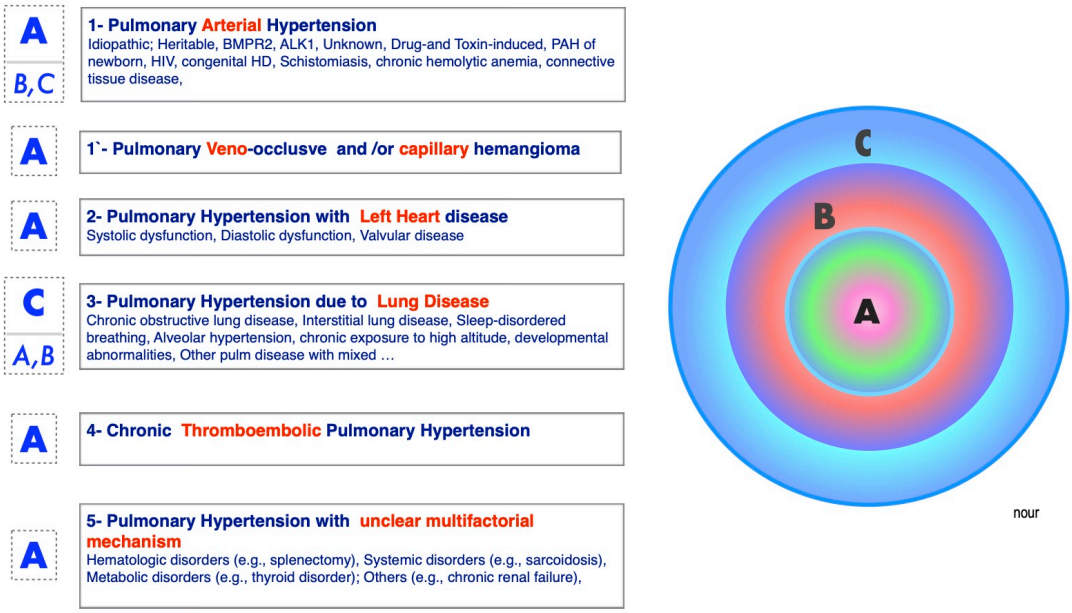
A
B,C
1- Pulmonary Arterial Hypertension
Idiopathic; Heritable, BMPR2, ALK1, Unknown, Drug-and Toxin-induced, PAH of newborn, HIV, congenital HD, Schistomiasis, chronic hemolytic anemia, connective tissue disease,
A
1`- Pulmonary Veno-occlusve and /or capillary hemangioma
A
2- Pulmonary Hypertension with Left Heart disease
Systolic dysfunction, Diastolic dysfunction, Valvular disease
C
A,B
3- Pulmonary Hypertension due to Lung Disease
Chronic obstructive lung disease, Interstitial lung disease, Sleep-disordered breathing, Alveolar hypertension, chronic exposure to high altitude, developmental abnormalities, Other pulm disease with mixed …
A
4- Chronic Thromboembolic Pulmonary Hypertension
A
5- Pulmonary Hypertension with unclear multifactorial mechanism
Hematologic disorders (e.g., splenectomy), Systemic disorders (e.g., sarcoidosis), Metabolic disorders (e.g., thyroid disorder); Others (e.g., chronic renal failure),
C
B
A
nour

Figures

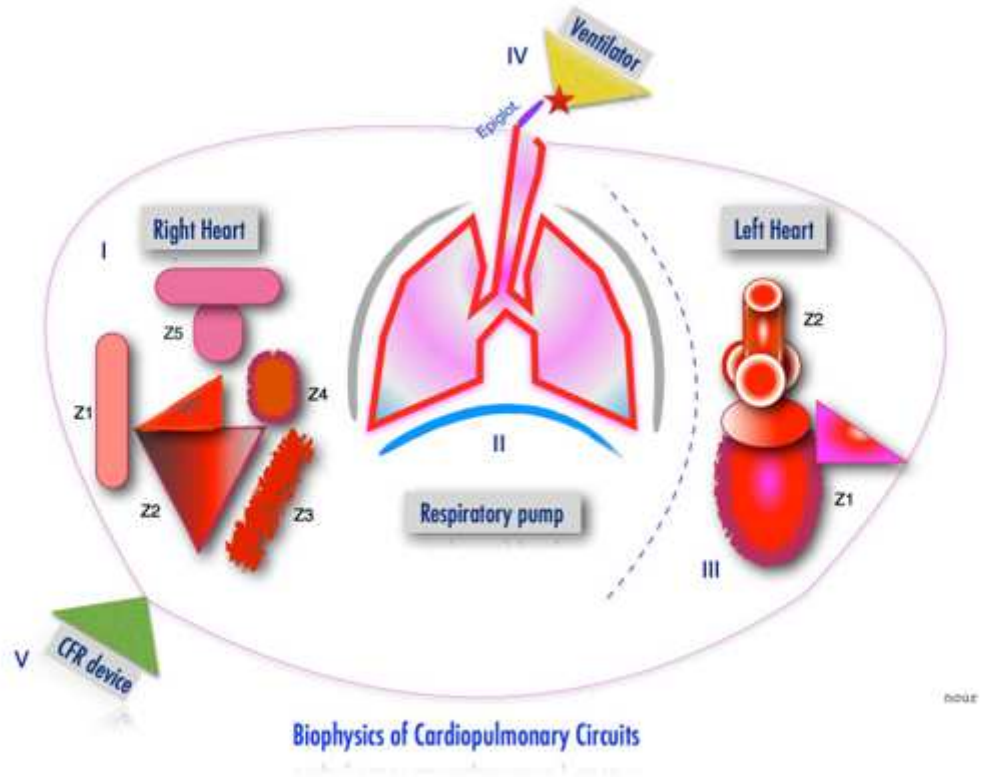

Figure 1

Biophysics of cardiopulmonary circulatory driving forces. I: Right heart circuit main remodeling zones: Z1, systemic veins; Z2, right ventricle; Z3, septum; Z4, infundibulum; Z5, pulmonary artery [ref.]. II: Respiratory pump; a semiclosed pressurized circuit that compresses two types of fluids: Newtonian (air) and non-Newtonian (blood), in an accordion-like manner, creating ESS. III: Left heart circuit main remodeling zones: Z1, left ventricle; Z2, Aorta & Valsalva. IV: Mechanical ventilator: creates a nonphysiological immobilized closed pressurized respiratory circuit with suppression of ESS. V: CFR device that could restore circulatory flow dynamics and maintain respiratory pump function. [Artif Organs, Vol. 41, No. 2, 2017].

Figure 2

Shows the Circulatory flow restoration (CFR) device in a suitcase (middle panel) that contains (right panel): Vest (T2), abdominal corset (T1) and Console of commands (G). Left panel: a wrapped device around a patient on a deployed medical stretcher suitcase.

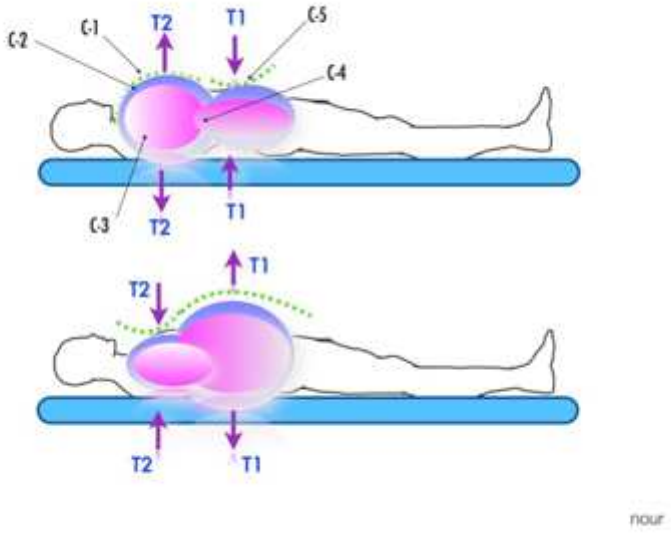

Figure 3

A schema representing the mechanism of the alternating compression/decompression the thoracic (T2) and abdominal (T1) compartments of the CFR device. The upper panel shows the CFR in an inspiration phase. The Lower panel shows the CFR in an expiration phase. C= covering endothelial layer shearing zone; C-1= thoracic cage; C-2= mediastinal shearing mass; C-3= pulmonary parenchyma, C-4= diaphragmatic pump; C-5 = hepatosplanchnic shearing mass.

Figure 4

Thoracic vest and trousers prototype wrapped around piglet body and connected to pneumatic generator [Artif Organs, Vol. 41, No. 2, 2017].

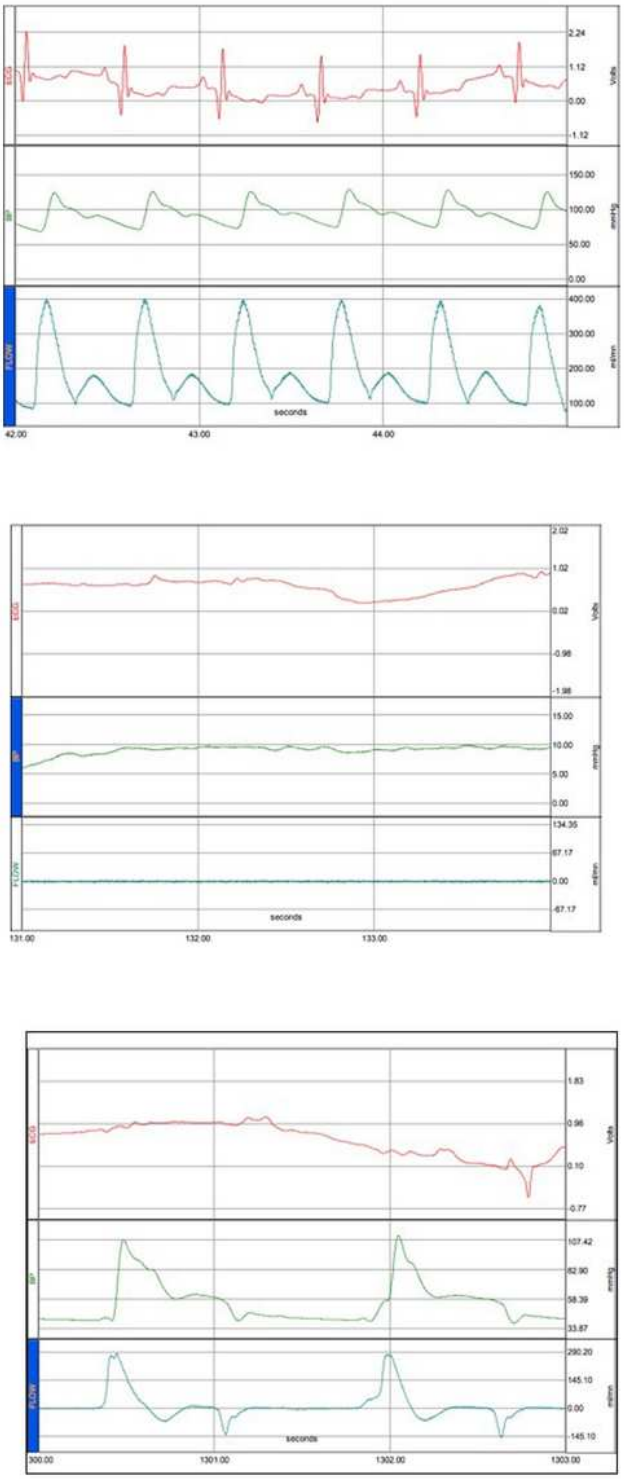

Figure 5

Figure 5A: Hemodynamic data obtained in a pediatric cardiac arrest model at baseline, showing ECG readings (upper line), aortic pressure line (middle curve) and carotid flow Figure 5B: Post cardiac arrest hemostatic data. Figure 5C: Restoration of hemodynamics with CFR device in a pediatric model after 30 min of cardiac arrest by asphyxia [Artif Organs, Vol. 41, No. 2, 2017].

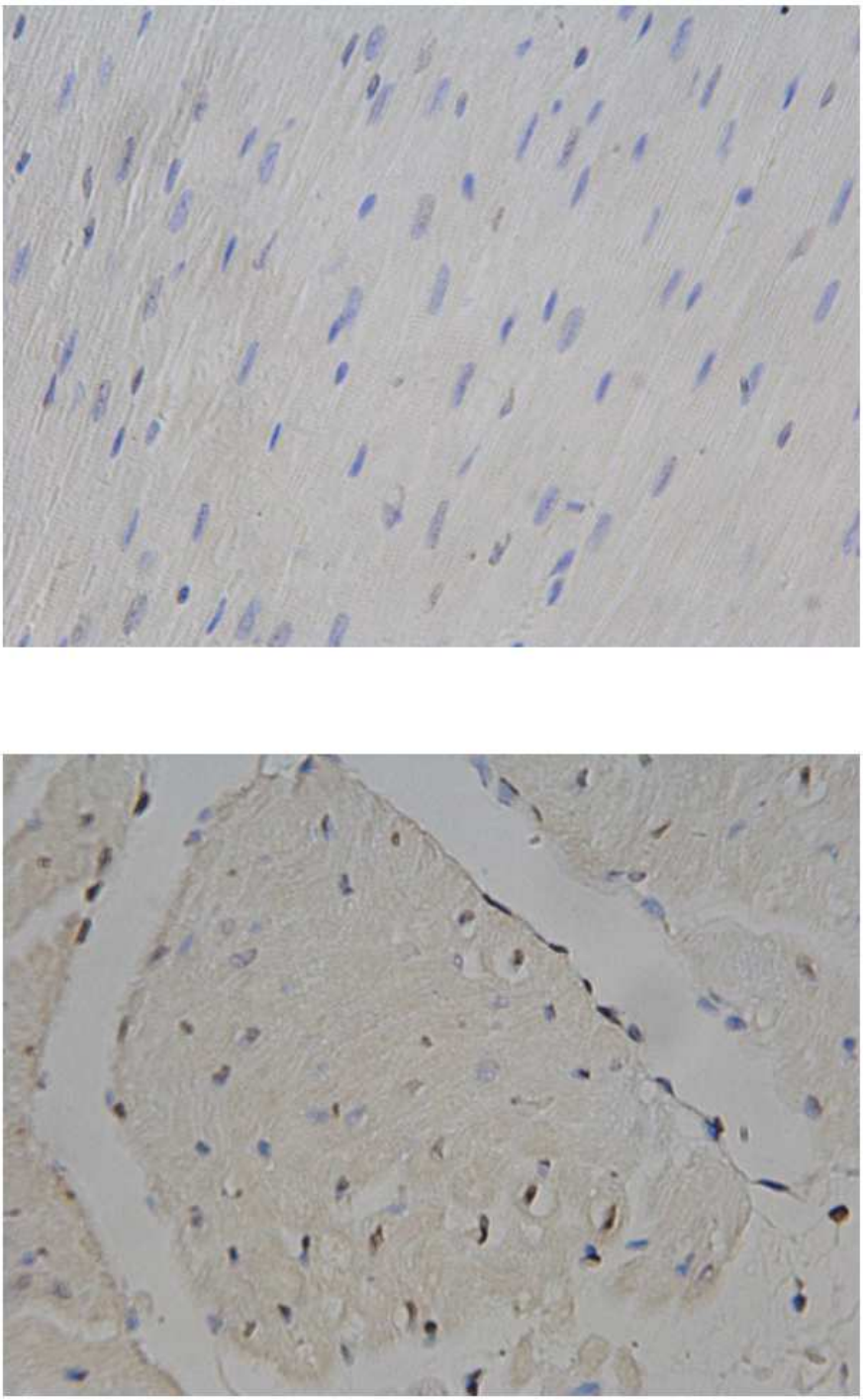

Figure 6

Figure 6A: TUNEL test showing manifestation of myocardial apoptotic cells (blue color) in control. Figure 6B: TUNEL test showing few manifestations of myocardial apoptotic cells (blue color) with vasodilation of intramyocardial vessels in tested in puppy (asphyxia model) after 2 h of device pulsations [Artif Organs, Vol. 41, No. 2, 2017].

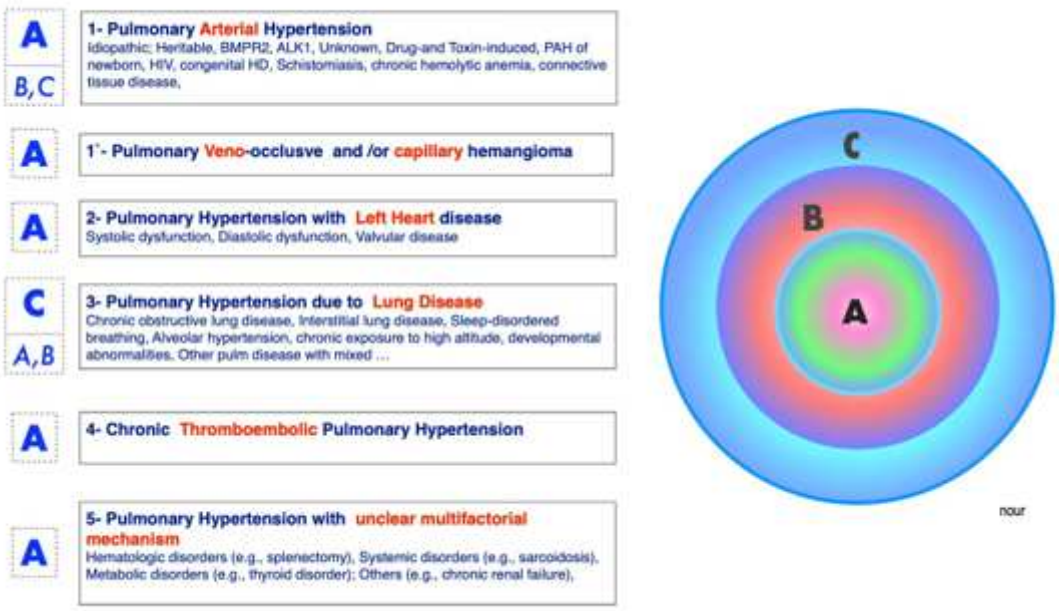

Figure 7

Dana Point vs. ABC Target-Board Pulmonary Hypertension Management [17]. Right panel: Schematic imaginary division of the human body into three rheological spheres (A, B and C): A = amount of fluid; B = barriers of cells; C = covering tissues; “Somarheology theory” [18]. Middle panel Dana Point PAH classification [47]. Left panel: mismatching the Dana Point groups of PAH & ABC spheres. Endothelial shear stress could be triggered at B, through A and/or C.

Supplementary Files

This is a list of supplementary files associated with this preprint. Click to download.

- Tables.docx